PHYSICAL REVIEW B **79**, 245131 (2009)

Origin of hysteresis in resistive switching in magnetite is Joule heating

A. A. Fursina,[1] R. G. S. Sofin,[2] I. V. Shvets,[2] and D. Natelson[3,4]
[1]*Department of Chemistry, Rice University, 6100 Main Street, Houston, Texas 77005, USA*
[2]*School of Physics, CRANN, Trinity College, Dublin 2, Ireland*
[3]*Department of Physics and Astronomy, Rice University, 6100 Main Street, Houston, Texas 77005, USA*
[4]*Department of Electrical and Computer Engineering, Rice University, 6100 Main Street, Houston, Texas 77005, USA*
(Received 17 April 2009; published 26 June 2009)

In many transition-metal oxides the electrical resistance is observed to undergo dramatic changes induced by large biases. In magnetite, Fe_3O_4, below the Verwey temperature, an electric-field-driven transition to a state of lower resistance was recently found, with hysteretic current-voltage response. We report the results of pulsed electrical conduction measurements in epitaxial magnetite thin films. We show that while the high- to low-resistance transition is driven by electric field, the hysteresis observed in *I-V* curves results from Joule heating in the low-resistance state. The shape of the hysteresis loop depends on pulse parameters and reduces to a hysteresis-free "jump" of the current provided thermal relaxation is rapid compared to the time between voltage pulses. A simple relaxation-time thermal model is proposed that captures the essentials of the hysteresis mechanism.

DOI: 10.1103/PhysRevB.79.245131 PACS number(s): 71.30.+h, 73.50.−h, 72.20.Ht

Dramatic changes in resistance induced by electric fields, so-called resistive switching (RS), have recently attracted much attention due to this phenomenon's potential application in memory devices (resistive random access memory).[1,2] RS from high- to low-resistance states is driven by application of high voltage and corresponding up-and-down sweeps of current-voltage (*I-V*) characteristics often show hysteresis, i.e., in sweeps up and down in bias voltage, the current does not retrace itself. Systems exhibiting hysteretic RS include organic compounds[3] and transition-metal oxides such as widely studied colossal resistance manganites,[4] perovskites (e.g., $SrTiO_3$),[5] one-dimensional cuprates Sr_2CuO_3,[6] NiO,[7] TiO_2 (Ref. 8), etc.

For some RS systems, while sweeping out a hysteresis loop in *I-V* with a switch to a low-resistance state at high bias, the low-resistance state persists down to zero current as voltage approaches zero. This behavior is often the case for RS systems where the switching is based on metallic filament formation at a transition point.[5] However, for some RS systems the low-resistance state persists only in some voltage interval and the system returns to the high-resistance state before voltage returns to zero. This is the case for some metal oxides[4,9–12] as well as for magnetite nanostructures, which were recently shown to exhibit RS at low temperatures.[13,14]

Magnetite, Fe_3O_4, is an example of strongly correlated material. In equilibrium, bulk magnetite undergoes a structural transition at the Verwey temperature, $T_V \sim 120$ K, accompanied by 3-order-of-magnitude change in electrical conductivity, i.e., a metal-insulator transition.[15] Recently we demonstrated that magnetite nanoparticles and thin films, once in the insulating state below T_V, exhibit RS under a sufficiently large voltage bias.[13] By examining RS systematically in different device geometries, the switching was demonstrated to be driven by the applied in-plane electric field. This is in contrast to previously observed transitions in magnetite driven by Joule heating of the samples above T_V under bias.[16,17] When the voltage is swept continuously, the electric-field-driven switching takes place at either polarity of voltage with well-pronounced hysteresis.

In this paper we determine the origin of hysteresis in magnetite structures based on epitaxial thin films. Through extensive voltage pulse measurements with controlled pulse parameters we unambiguously show that, while the high-resistance to low-resistance switching is driven by electric field, the hysteretic behavior originates from local Joule heating of the channel once the system is switched to the low-resistance state. A very simple thermal model agrees with the data with appropriately chosen parameters. The parameter values required to achieve quantitative consistency with the data demonstrate that one must consider heating and thermal transport beyond just the magnetite film itself.

Epitaxial magnetite thin films with 50 nm thickness were grown on ⟨100⟩ MgO single-crystal substrates by oxygen-plasma-assisted molecular-beam epitaxy. Details of the growth process have been reported elsewhere.[18,19] The films were characterized by reflection high-energy electron diffraction (*in situ* during growing), high-resolution x-ray diffraction measurements, Raman spectroscopy, and resistance measurement to prove crystalline quality and stoichiometry of the samples.[20,21] The films show a jump in the temperature dependence of resistance at $T \sim 108$ K [Fig. 1(a) inset], characteristic of the Verwey transition in magnetite thin films.

Devices for two-terminal measurements were prepared by electron-beam lithography. A channel length of 190–900 nm is defined by two 5–10 μm-wide current leads [Fig. 1(a) inset], which are connected to micrometer-size pads (300 $\times$ 300 μm). Upon testing several different contact metals (Au, Pt, Cu, Fe, and Al), copper showed the lowest contact resistance with the magnetite film. Thus, the electrodes were made of 6-nm-Cu/15-nm-Au thin layers deposited by electron-beam evaporation.

Electrical characterization of the samples was performed by a standard two-terminal method using a semiconductor parameter analyzer (Hewlett Packard 4155A). The voltage

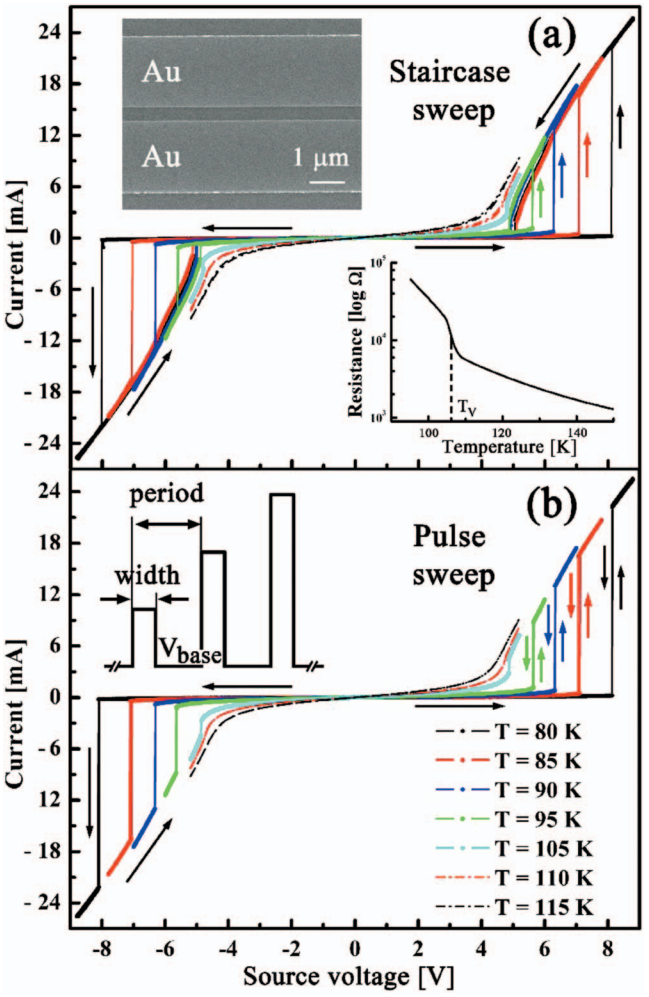

FIG. 1. (Color) Typical *I-V* curves at different temperatures in (a) continuous staircase and (b) pulse sweep modes. Arrows indicate the direction of voltage sweeps. Above a certain temperature (in this case ~105 K) sharp jumps in current are not observable. Top (a) inset shows a scanning electron micrograph of a two-terminal device on the surface of a magnetite film; bottom (a) inset shows a temperature dependence of resistance demonstrating Verwey transition at $T_V \sim 108$ K. The (b) inset schematically represents the pulse parameters for the pulsed sweeps. Successive applied voltages differ by 1–15 mV depending on the total sweep range.

was applied to the source lead with the drain grounded and current flowing through the channel was monitored. Two different measurement methods were used: a continuous staircase sweep of the source voltage up and down and a pulsed sweep implemented with controlled pulse parameters. Each voltage sweep consists of 1000 points equally spaced in voltage. Measurements were performed in the temperature range of 80–300 K with 5 K steps.

At high temperatures *I-V* curves have a slightly nonlinear shape [Figs. 1(a) and 1(b)] typical for many transition-metal oxides. Below a certain temperature, coincident with the Verwey temperature inferred from measurements of the zero-bias resistance, a sharp jump in current was observed as the source voltage reached a critical value, as described previously.[13] At 80 K, for example, the current changes abruptly by a factor of 100 at a particular switching voltage. The state after transition ("On" state) shows an approximately linear *I-V* dependence with a much smaller differential resistance than that of high-resistance ("Off") state prior to the transition. At a given temperature and device geometry, the switching happens at a critical voltage, V_{sw}^{On}, and as the voltage is swept back the system remains in the On state until it switches back to the Off state at a switch-off voltage V_{sw}^{Off}. For a continuous staircase sweep V_{sw}^{Off} is always lower than V_{sw}^{On}, resulting in a well-defined hysteresis [Fig. 1(a)]. The transition is symmetrical along *V* axis with identical transitions occurring at positive and negative voltage sweeps.

Switching phenomena are observed at temperatures right below Verwey temperature (~108 K) and, thus, magnetite is comparatively insulating in the undisturbed state [see zero-bias *R* vs *T* dependence in Fig. 1(a) inset]. Previously we demonstrated that the observed transition is driven by electric field and not by thermal heating of the magnetite sample above Verwey temperature.[13] In the high-resistance state ($|V| < V_{sw}^{On}$) heating of the sample is comparatively negligible, whereas in the On state dissipated power significantly increases, making Joule heating of the sample much more likely. Below we use pulsed measurements to demonstrate that this On state heating is the origin of the apparent hysteretic behavior in our system.

We performed pulsed sweep experiments, with controlled duration of the voltage pulse (pulse width), the time between consecutive pulses (pulse period) and the voltage value at rest between the pulses (base voltage) [Fig. 1(b) inset]. In these pulsed measurements the base voltage may be kept $V_{base}=0$ V eliminating Joule heating and allowing cooling of the channel between pulses. The dependence of system response on pulse width and pulse period can indicate heating dynamics of the sample (especially in the On state).

First, we investigated the system response to pulse sweeps with different *widths*: we varied the pulse duration while keeping fixed the time system stays at the base voltage [(pulse period) - (pulse width) = const ($V_{base}=0$ V), see Fig. 1(b) inset]. Figure 2(a) shows resultant *I-V* curves (only positive voltages for better visualization) at 80 K. The shape of the hysteresis clearly changes as pulse width increases: V_{sw}^{Off} moves farther away from V_{sw}^{On}, which remains independent of the pulse width [Fig. 2(a)]. Note that the current is consistently higher for longer pulses.

In a second set of pulse experiments we made voltage sweeps with various pulse *periods* and constant pulse width. One of the shortest possible pulse widths (0.5 ms or 1 ms in our setup) was used to minimize heating of the sample. The increase in pulse period has an opposite effect on V_{sw}^{Off} position than the increase in pulse width: V_{sw}^{Off} moves closer to V_{sw}^{On} as the pulse period increases [Fig. 2(b)], i.e., as the system rests at zero-bias voltage between pulses for longer times. Note, again, that V_{sw}^{On} position remains independent of pulse period. At long enough period times (>100 ms) V_{sw}^{On} and V_{sw}^{Off} are of the same value. Figure 1(b) shows *I-V* curves at different temperatures obtained by pulse sweeps with a 100 ms pulse period. Instead of hystereses there are sharp jumps in On state and back to Off state at almost the same voltage: $V_{sw}^{Off} \approx V_{sw}^{On}$.

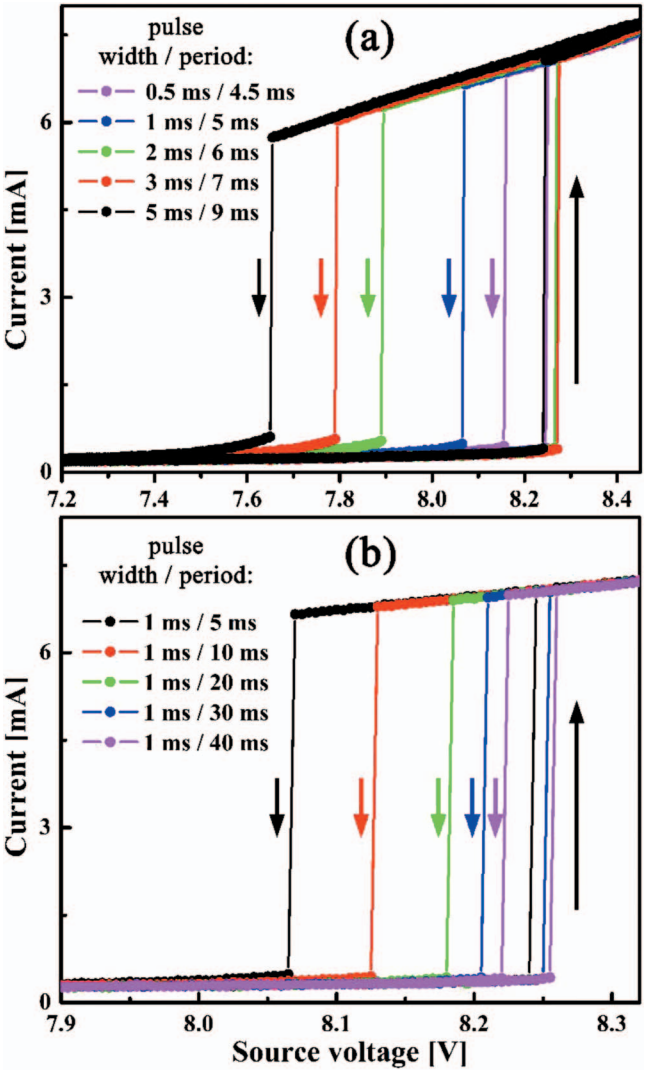

FIG. 2. (Color) Dependence of hysteresis (I-V curve) shape at 80 K in pulse sweep mode on (a) pulse width, while the time sample rests at V_{base} is kept constant (4 ms) and (b) pulse period, while pulse width is kept the same (1 ms). Base voltage, V_{base}, is always set to 0 V.

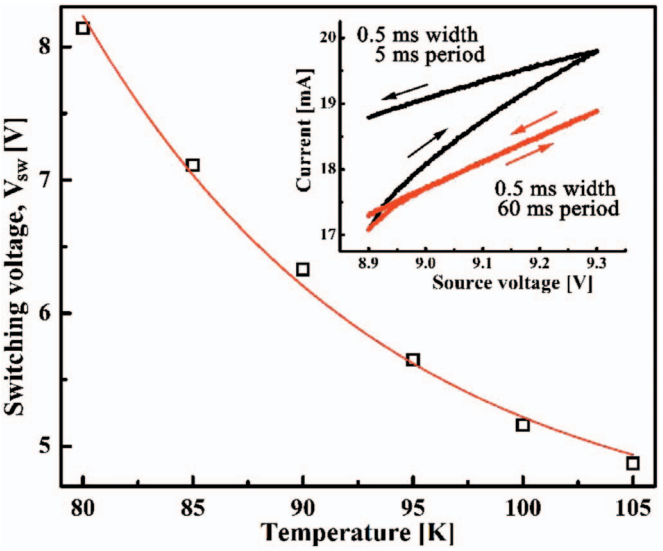

FIG. 3. (Color) Temperature dependence of switching voltage (open squares) and its exponential fit (solid line). The inset shows I-V curves in the On state in pulse sweep mode with the same pulse width (0.5 ms) but different pulse periods showing that rapid pulse repetition leads to more severe heating, as expected.

While hysteretic RS (with differentiated V_{sw}^{On} and V_{sw}^{Off} values) was previously observed in many systems, here we demonstrate that in magnetite there is a single *intrinsic* switching value, $V_{sw}=V_{sw}^{On}=V_{sw}^{Off}$, and no intrinsic hysteresis. Thus, the switching voltage is a characteristic parameter of the system: at every temperature and device geometry, there is a certain switching voltage required to drive the transition. This V_{sw} decreases as temperature approaches T_V following a nearly exponential dependence (Fig. 3). The separation of V_{sw}^{On} and V_{sw}^{Off} values, shifting of V_{sw}^{Off} position in sweeps with different pulse widths and periods, and the observation of hysteresis are easily explained by heating of the sample in the On state.

We first give a qualitative picture of how On-state heating leads to hysteresis and then provide a quantitative description with a simple model of channel temperature during a pulse sweep. The sample begins at an initial temperature T_{set}; for this temperature and a given channel length, there is a corresponding switching voltage, $V_{sw}(T_{set})$ (Fig. 3). Consider performing a sweep with pulse parameters selected to give hysteresis. First, as we start sweeping voltage from 0 V up, the system remains approximately at T_{set} prior to the transition point due to the comparatively small amount of Joule heating. After application of a pulse with $V>V_{sw}(T_{set})$, the system is driven into the On state. With the resulting increased conductance (and, thus, current) the Joule heating of the channel is much larger, elevating the local effective temperature of the channel to $T_{cur}>T_{set}$. Non-steady-state warming of the sample continues further in the On state. This is clear from the nonlinear increase in the current and the fact that the I-V trace in the On state does not retrace itself (Fig. 3 inset). Note that sufficiently increasing the pulse period does allow I-V curves to retrace themselves on up and down sweeps (Fig. 3 inset). As the pulse voltage is swept back below $V_{sw}(T_{set})$, the channel remains in the On state because the channel is at the elevated effective temperature, T_{cur}, and the switching voltage is therefore lower: $V_{sw}(T_{cur})<V_{sw}(T_{set})$.

If the channel cools down to T_{set} between two consecutive pulses, the system remains in the Off state for any voltage applied that is lower than $V_{sw}(T_{set})$ and jumps are observed instead of hysteresis [Fig. 1(b)]. If the pulse period is short compared to the thermal relaxation time, then the channel remains at $T_{cur}>T_{set}$, and we observe the separation of $V_{sw}^{On}=V_{sw}(T_{set})$ and $V_{sw}^{Off}=V_{sw}(T_{cur})$, and resulting hysteresis. Upon increasing the pulse period (system stays longer at $V_{base}=0$ V), the channel has more time to cool after application of previous pulses, T_{cur} is closer to T_{set}, and V_{sw}^{Off} moves closer to V_{sw}^{On} in excellent agreement with the experimental data [Fig. 2(b)]. In experiments on increasing pulse widths, it is clear that longer pulses heat the channel more than shorter pulses, thus T_{cur} is higher in the former case, corresponding to lower $V_{sw}(T_{cur})$. Thus, experimentally ob-

served moving V_{sw}^{Off} away from V_{sw}^{On} as the pulse width increases [Fig. 2(a)] is completely consistent with this heating picture.

As qualitatively described above, V_{sw}^{Off} position is related to the current local temperature of the channel. To quantitatively describe the movement of V_{sw}^{Off} position in sweeps with different pulse parameters, we should consider a model to estimate the effective channel temperature as a function of applied pulsed voltage (and time). Detailed thermal modeling is very challenging because of the highly local character of the heating and the difficulty of capturing all the relevant heat transfer processes in these nanostructures. Instead we consider a simple model where the return to equilibrium state (relaxation) is described by a relaxation time, τ,[22] and the temperature change is

$$\frac{\partial T}{\partial t}(\text{relaxation}) = -\frac{T - T_{set}}{\tau}, \tag{1}$$

where T is a current temperature of the channel. The heat flux into the sample is obviously $dQ_{in}/dt = V \times I$. We further assume that the heat dissipation can be simply described as

$$\frac{dQ_{out}}{dt} = -C_v \frac{T - T_{set}}{\tau}, \tag{2}$$

where C_v is a heat capacity of the sample (in J/K).

Note that this model assumes C_v and τ to be independent of temperature, which is clearly an idealization. The temperature variation with respect to time, $\partial T/\partial t$, considering total heat flux through the system, i.e., $\frac{\partial}{\partial t}(Q_{in}+Q_{out})$, is given by

$$C_v \frac{\partial T}{\partial t} = \frac{\partial}{\partial t}(Q_{in} + Q_{out}) = V \times I - C_v \frac{T - T_{set}}{\tau}. \tag{3}$$

By solving Eq. (3) we derive an expression for a temperature, $T(t+dt)$, given the current temperature, $T(t)$, in a moment of time, dt:

$$T(t + dt) = T_{set} + \frac{V \times I \times \tau}{C_v}\left[1 - \exp\left(-\frac{dt}{\tau}\right)\right] + [T(t) - T_{set}]\exp\left(-\frac{dt}{\tau}\right). \tag{4}$$

When $V \neq 0$, both heating and cooling (by relaxation to equilibrium T_{set}) processes occur described by second and third terms of the right side of Eq. (4), respectively. Between pulses ($V_{base}=0$ V) only heat dissipation takes place and Eq. (4) reduces to the expected exponential decay of the temperature with the relaxation time, τ, as a scaling factor

$$T(t + dt) = T_{set} + [T(t) - T_{set}]\exp\left(-\frac{dt}{\tau}\right). \tag{5}$$

There are two fitting parameters in this model that govern the evolution of the current temperature: heat capacity C_v and relaxation time τ.

An example of T variation calculated by Eq. (4) is shown in Fig. 4 with real experimental data for sourced voltage, V, and measured current, I (sweep with 3 ms pulse duration and 7 ms pulse period), and C_v and τ values as will be discussed below. Figures 4(a) and 4(b) show the calculated temperature of the channel as a function of source voltage and corresponding time, respectively, over a large voltage range around transition point. Black points represent T values before the transition to the On state and they do not deviate much from T_{set} (80 K in this case). As the system is switched to the On state the temperature profile changes drastically: as pulse voltage is sourced, T increases and blue triangles show the calculated T values right after pulse application ("high-T" state). After relaxation for a time between pulses, the channel cools down to temperatures represented by red circles ("low-T" state), which are only slightly higher than original T_{set}. For better visualization, Fig. 4(c) zooms into the small region indicated by the hatched area in Fig. 4(b) at a turning point of a sweep (from sweep up to sweep down in voltage). It clearly demonstrates how the temperature first rapidly rises as the pulse is applied and then decreases as the system rests at $V_{base}=0$ V (shaded regions), relaxing back toward $T_{set}=80$ K. Both high-T and low-T temperatures follow the applied voltage: T increases as V is swept up and starts decreasing as sweep is reversed and V decreases [follow the red circles and blue rectangles in the bottom of Fig. 4(c)].

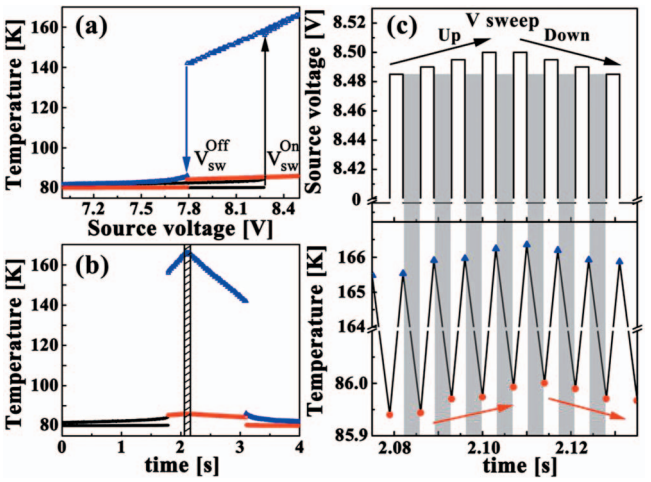

FIG. 4. (Color) Calculated temperature in relaxation-time model [see Eq. (4)] with respect to (a) source voltage and (b) corresponding time for a voltage pulse sweep with 3 ms pulse duration and 7 ms pulse period. Black points reflect T values before the transition point $V < V_{sw}$. After the transition point, blue triangles show T immediately after pulse application and red circles show T after relaxation between two sequential pulses. The hatched area in (b) indicates the time interval depicted in detail in (c). Applied pulsed voltage as a function of time (top) with corresponding calculated temperature of the channel (bottom). Shaded areas indicate time intervals when system is not under bias (i.e., source voltage is zero) and only relaxation to T_{set} is taking place [see Eq. (5)].

Each device has its defined single-valued $V_{sw}(T)$ function (an example is shown in Fig. 3) with V_{sw} being a characteristic parameter at a certain temperature. During a voltage sweep *down*, the temperature at the moment the pulse is applied decreases [follow the red circles in Fig. 4(c)] while V_{sw} corresponding to this temperature increases. Note that when the pulse voltage is applied the relevant temperature is that of the low-T state [red circles in the bottom of Fig. 4(c)],

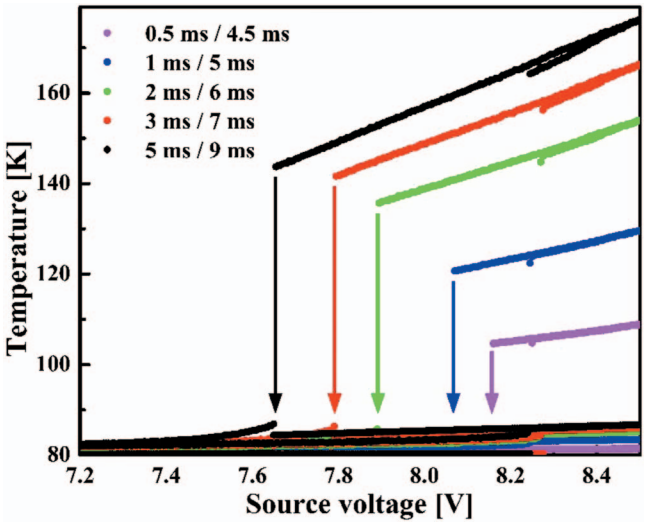

FIG. 5. (Color) The dependence of calculated temperature on source voltage in the relaxation-time model for sweeps with different pulse widths and the same time between pulses (4 ms) T_{set} =80 K. High-T (immediately after pulse application) and low-T (after relaxation between pulses) state temperatures are plotted in the same color, with the latter apparent at the bottom of the figure. Arrows indicate switching back position for each sweep, which happens when applied voltage becomes lower than V_{sw} for a current temperature of the channel.

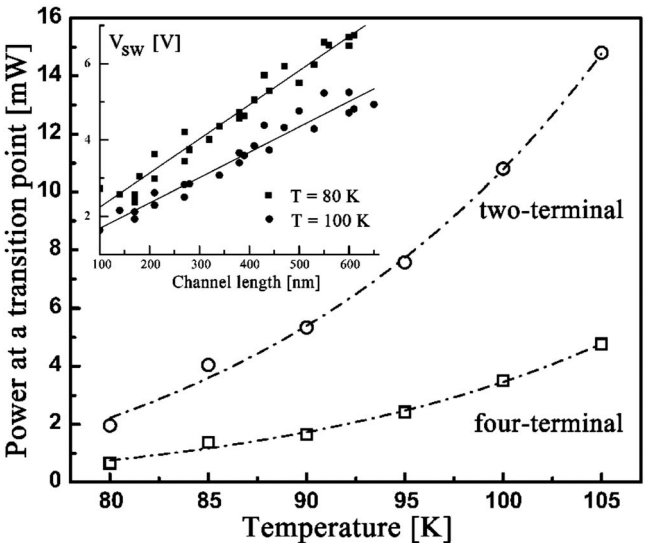

FIG. 6. Temperature dependence of the power at a transition point, V_{sw}^{On}, in two-terminal ($P_{sw}^{2T}=V\times I$) and four-terminal ($P_{sw}^{4T}=\Delta V\times I$) experiments. Inset shows the dependence of the two-terminal switching voltage, V_{sw}, on the channel length at two different temperatures. Solid lines represent a linear fit; the slope of each line reflects the electric-field strength required to drive the transition.

thermally relaxed after application of the preceding pulse. Switching from On to Off states happens as soon as applied pulse V value is lower than V_{sw} for the *current* temperature of the channel at the time the pulse is applied.

We find that the proposed model can match experimental V_{sw}^{Off} positions with appropriately chosen C_v and τ values. For each device at a given T_{set} we can find a C_v and τ pair that accurately describes the shifting of V_{sw}^{Off} position for sweeps with different pulse widths and the same time between pulses (pulse period) - (pulse width) = const. An example of temperature dependence on applied pulsed voltage is shown in Fig. 5 corresponding to the experimental I-V curves in Fig. 2(a). The adjusted optimum values of C_v and τ are 10^{-6} J/K and 1.5×10^{-3} s, respectively.

To get a sense of what these parameter values imply, we note that the estimated heat capacity value based on specific heat capacity and density of magnetite [$C_v\sim40$ J/(mol K) at 80 K,[23] $\rho=5.18$ g/cm^3] and geometrical parameters of the channel is $\sim10^{-13}$ J/K. This is much lower than the C_v value required by the model to match the observed trends strongly implying that heating is not confined only to the channel but involves a much larger volume. This also implies that the MgO substrate and Au electrodes are relevant to the thermal relaxation process.

For sweeps with different pulse periods and the same pulse width, V_{sw}^{off} positions cannot be satisfactory modeled with a single C_v and τ pair. For a fixed C_v, sweeps with longer pulse periods demand larger τ values to match the experimentally observed V_{sw}^{off} positions. Longer period times imply larger temperature variation over the time relaxation process takes place [see Eq. (5)]. This is almost certainly due to the failure of the idealized assumption of C_v and τ being independent of temperature. A much more sophisticated thermal model (incorporating the spatial temperature distribution and the temperature-dependent thermal properties of the magnetite, the substrate, and the electrodes) is likely necessary for a complete quantitative picture.

Since heating effects in the On state are responsible for hysteresis in this system, it is worthwhile to review the arguments that the high-resistance to low-resistance transition itself is *not* driven by heating the sample above Verwey temperature, but indeed is driven by electric field.[13] First, a strong argument against heating effect is the temperature dependence of the power, P_{sw}, dissipated at the transition point. It was shown in Ref. 13 for two-terminal devices that $P_{sw}^{2T}=V\times I$ at V_{sw}^{On} decreases as temperature decreases. This behavior is incompatible with the assumption that raising of the channel temperature above Verwey temperature (here $T_V\sim108$ K) is responsible for the resistance switching. Assuming a heating effect, the lower the set temperature the more power should be provided to warm up a channel above T_V, the opposite of the trend observed in the experiment. In this work we confirm the P_{sw} vs T dependence in the two-terminal geometry (Fig. 6). Additionally, we performed four-terminal measurements (details to be given separately in Ref. 24) and calculated the corresponding local switching power dissipated in the channel, $P_{sw}^{4T}=\Delta V\times I$ at a transition point, where ΔV is a voltage difference between two voltage probes within the channel. P_{sw}^{4T} is much lower than P_{sw}^{2T} because of the significant contact voltage drop at the electrode/Fe_3O_4 interface. The power dissipated directly in the channel, P_{sw}^{4T}, shows the same temperature dependence as P_{sw}^{2T} (Fig. 6), arguing further against simple heating driving the transition.

A second argument for that the transition is electrically driven is the dependence of V_{sw} on the length of the channel.

At each temperature V_{sw} scales *linearly* with the channel length, L (Fig. 6 inset). This implies that at each temperature there is a certain electric field necessary to drive a transition. Extracted from the slope of V_{sw} vs L, the critical electric-field value is about 7×10^4 V/cm at 105 K and it increases slightly up to $\sim10^5$ V/cm down to 80 K (Fig. 6 inset). These values are much lower than the catastrophic dielectric breakdown field ($\sim10^7$ V/cm) (Ref. 25) for most insulators.

Third, pulse experiments that widely span heating conditions show no shift in V_{sw} position upon varying either pulse width or pulse period. Longer pulses deliver more energy to the channel [$=I\times V\times t$, where t is the duration (width) of the pulse]. Assuming a thermal switching mechanism, the switching would be expected at lower voltages for longer pulses, which is not the case in the experiments. Different pulse widths and periods have tremendous effects (both in V_{sw}^{Off} positions and current values) on the behavior of the system in the On state (Fig. 2) when heating is clearly an issue. In the Off state only minor changes in *I-V* curves were detectable for sweeps with all available widths and periods. Finally, sourcing a constant voltage for minutes right below V_{sw} value at a certain temperature does not induce or alter the transition.

In conclusion, resistive switching in magnetite thin films from a high-resistance state to a low-resistance state is driven by an electric field, while the hysteresis observed in such switching is a result of thermal effects. We find that a simple relaxation-time model of the thermal processes can describe the shifting of V_{sw}^{off} positions for sweeps with different pulse parameters. Model parameters indicate that the substrate and electrodes are important in determining the thermal dynamics of the system. The electric-field-driven switching observed in magnetite is different than several mechanisms suggested for RS in perovskites such as dynamics of oxygen vacancies and interfacial effects. First, the lack of intrinsic hysteresis differentiates magnetite RS from that in the perovskites. Second, magnetite RS can be induced only *below* the Verwey temperature, T_V, whereas RS in perovskites is observed in a wide range of temperatures.[5] Below T_V magnetite is in a correlated ordered state.[26,27] Thus, RS in Fe_3O_4 is a strong candidate for the theoretically predicted breakdown of *charge-ordered* states by electric field.[28] The mechanism of this nonequilibrium transition demands further investigation.

This work was supported by the U.S. Department of Energy under Grant No. DE-FG02-06ER46337. D.N. also acknowledges the David and Lucille Packard Foundation and the Research Corporation. R.G.S.S. and I.V.S. acknowledge the support of Science Foundation of Ireland under Grant No. 06/IN.1/I91.

[1] A. Sawa, Mater. Today **11**, 28 (2008).
[2] R. Waser and M. Aono, Nature Mater. **6**, 833 (2007).
[3] R. Müller, R. Naulaerts, J. Billen, J. Genoe, and P. Heremans, Appl. Phys. Lett. **90**, 063503 (2007).
[4] A. Asamitsu, Y. Tomioka, H. Kuwahara, and Y. Tokura, Nature (London) **388**, 50 (1997).
[5] K. Szot, W. Speier, G. Bihlmayer, and R. Waser, Nature Mater. **5**, 312 (2006).
[6] Y. Taguchi, T. Matsumoto, and Y. Tokura, Phys. Rev. B **62**, 7015 (2000).
[7] D. C. Kim, S. Seo, S. E. Ahn, D.-S. Suh, M. J. Lee, B.-H. Park, I. K. Yoo, I. G. Baek, H.-J. Kim, E. K. Yim, J. E. Lee, S. O. Park, H. S. Kim, U-In. Chung, J. T. Moon, and B. I. Ryu, Appl. Phys. Lett. **88**, 202102 (2006).
[8] B. J. Choi, D. S. Jeong, S. K. Kim, C. Rohde, S. Choi, J. H. Oh, H. J. Kim, C. S. Hwang, K. Szot, R. Waser, B. Reichenberg, and S. Tiedke, J. Appl. Phys. **98**, 033715 (2005).
[9] C. Li, X. Zhang, Z. Cheng, and Y. Sun, Appl. Phys. Lett. **93**, 152103 (2008).
[10] L. J. Zeng, H. X. Yang, Y. Zhang, H. F. Tian, C. Ma, Y. B. Qin, Y. G. Zhao, and J. Q. Li, Europhys. Lett. **84**, 57011 (2008).
[11] M. Ovaida, B. Sacépé, and D. Shahar, Phys. Rev. Lett. **102**, 176802 (2009).
[12] B. L. Altshuler, V. E. Kravtsov, I. V. Lerner, and I. L. Aleiner, Phys. Rev. Lett. **102**, 176803 (2009).
[13] S. Lee, A. Fursina, J. T. Mayo, C. T. Yavuz, V. L. Colvin, R. G. S. Sofin, I. V. Shvets, and D. Natelson, Nature Mater. **7**, 130 (2008).
[14] A. Fursina, S. Lee, R. Sofin, I. Shvets, and D. Natelson, Appl. Phys. Lett. **92**, 113102 (2008).
[15] E. Verwey, Nature (London) **144**, 327 (1939).
[16] P. J. Freud and A. Z. Hed, Phys. Rev. Lett. **23**, 1440 (1969).
[17] T. Burch, P. P. Craig, C. Hedrick, T. A. Kitchens, J. I. Budnick, J. A. Cannon, M. Lipsicas, and D. Mattis, Phys. Rev. Lett. **23**, 1444 (1969).
[18] S. K. Arora, H.-C. Wu, H. Yao, W. Y. Ching, R. J. Choudhary, I. V. Shvets, and O. N. Mryasov, IEEE Trans. Magn. **44**, 2628 (2008).
[19] Y. Zhou, X. Jin, and I. V. Shvets, J. Appl. Phys. **95**, 7357 (2004).
[20] A. Koblischka-Veneva, M. R. Koblischka, Y. Zhou, S. Murphy, F. Muücklich, U. Hartmann, and I. V. Shvets, J. Magn. Magn. Mater. **316**, e663 (2007).
[21] S. K. Arora, R. G. S. Sofin, I. V. Shvets, and M. Luysberg, J. Appl. Phys. **100**, 073908 (2006).
[22] S. Volz, *Microscale and Nanoscale Heat Transfer* (Springer-Verlag, Berlin, 2007).
[23] J. P. Shepherd, J. W. Koenitzer, R. Aragón, C. J. Sandberg, and J. M. Honig, Phys. Rev. B **31**, 1107 (1985).
[24] A. A. Fursina, R. G. S. Sofin, I. V. Shvets, and D. Natelson (unpublished).
[25] J. McPherson, J. Kim, A. Shanware, H. Mogul, and J. Rodriguez, IEEE Trans. Electron Devices **50**, 1771 (2003).
[26] D. J. Huang, H.-J. Lin, J. Okamoto, K. S. Chao, H.-T. Jeng, G. Y. Guo, C.-H. Hsu, C.-M. Huang, D. C. Ling, W. B. Wu, C. S. Yang, and C. T. Chen, Phys. Rev. Lett. **96**, 096401 (2006).
[27] R. J. Goff, J. P. Wright, J. P. Attfield, and P. G. Radaelli, J. Phys.: Condens. Matter **17**, 7633 (2005).
[28] N. Sugimoto, S. Onoda, and N. Nagaosa, Phys. Rev. B **78**, 155104 (2008).